IEEE Access
Multidisciplinary | Rapid Review | Open Access Journal

Received June 15, 2020, accepted July 6, 2020, date of publication July 10, 2020, date of current version July 23, 2020.

Digital Object Identifier 10.1109/ACCESS.2020.3008455

Path Tracking Control of an Articulated Road Roller With Sideslip Compensation

MENG YANG[1], YONGMING BIAN[2], GUANGJUN LIU[2], AND HAO ZHANG[1]
[1]Department of Control Science and Engineering, Tongji University, Shanghai 201804, China
[2]School of Mechanical Engineering, Tongji University, Shanghai 201804, China

Corresponding author: Yongming Bian (ymbianmail@tongji.edu.cn)

This work was supported in part by the National Postdoctoral Program for Innovative Talents of China under Grant BX20190242, in part by the National Natural Science Foundation of China under Grant 71871160, and in part by the National Key Research and Development Program of China under Grant 2016YFC0802900 and Grant 2017YFE0100900.

ABSTRACT Unmanned road roller has become an attractive solution to reduce operators' working intensity and improve compaction efficiency. As a result of working in bumpy environments, sideslip effect is unavoidable during the compacting process. In order to guarantee the reliability and stability of path tracking control, a novel and effective method based on preview control and sideslip compensation is proposed in this paper. The kinematic and dynamic models of articulated road roller considering sideslip angles are obtained first. Then, a preview controller with sideslip compensation (PCSC) is developed to eliminate the path tracking errors between the actual path and the desired path. To evaluate the control performance of the proposed method, simulation under the MATLAB/Simulink and automatic compaction experiments at the construction site were performed with initial errors. Finally, the simulation and experimental results show that the path tracking errors can converge to zero as time goes by. The proposed method has the ability to navigate an articulated road roller to track a desired path in the existence of sideslip, only regarding the steering angle dynamic as control input. Compared with other benchmark method, it not only improves the control accuracy, but also increases the convergence rate, proving its effectiveness and feasibility. All these also demonstrate the practical value and validity of the proposed models with sideslip.

INDEX TERMS Path tracking, articulated road roller, sideslip compensation, preview control.

I. INTRODUCTION

As a typical compact machinery for earth-rock filling, road roller has played a significant role in constructing dams, airports, roadbeds and so on [1]–[3]. With the rapid development of filling engineering, the service condition of road roller is affected by some adverse external factors, such as large filling quantity, extreme construction environment and long uninterrupted working time. To reduce operators' working intensity and improve compaction efficiency simultaneously, unmanned road roller has become an attractive solution, depending on its obvious advantages.

Path tracking is one of the most elemental and important problems in the research of unmanned road roller, whose purpose is to ensure the vehicle can lock into a desired path with a designed control law [4]–[6]. It is important to point out that a road roller is an articulated steering type vehicle, which has two frames (front and rear) articulated by an active revolute joint. Its steering action is obtained by changing the angle between the front and rear frames, contributing to a better curve negotiation performance. Unfortunately, the active revolute joint brings additional degrees of freedom, which results in weakening the lateral stiffness of the vehicle and increasing the difficulty in control [7]–[9].

In the past years, numerous studies have been published concerning the path tracking control of articulated vehicles, especially tractor-trailer vehicles. Yue *et al.* [10] designed a posture controller based on model predictive control (MPC) to track the forward and backward obstacle avoidance maneuvers for tractor-trailer system. Khalaji [11] proposed a novel PID-based kinematic controller as a non-model-based controller to navigate the tractor-trailer wheeled robot follows desired trajectories. In [12], a varying time state feedback controller was designed to generate actuator torque by using Backstepping technique and Lyapunov direct method. Shao *et al.* [13] developed a path tracking strategy for the

The associate editor coordinating the review of this manuscript and approving it for publication was Zhixiong Peter Li.

articulated steering vehicles, where the reinforcement learning method was selected for optimizing the parameters of the PID algorithm to reduce control overshoot and oscillation. In [14], a coordinated control approach combining MPC and global terminal sliding mode control was presented for tractor–trailer vehicles, achieving a satisfactory trajectory tracking performance. Furthermore, the nonlinear kinematic model, and dynamic model under variable load and robust control with complex constraints of a tractor-trailer have been reviewed and discussed in [15]–[17]. However, it is noted that a tractor and a trailer are articulated by a rigid free joint. From the viewpoint of kinematics, each body has its own instantaneous center of velocity, which is different from articulated road roller. Path tracking control of a tractor-trailer depends on the trailer's motion with respect to the tractor. Therefore, these mentioned models and control laws of tractor-trailer cannot be directly used for articulated road roller.

Some authors also have examined the control theory of Load-haul-dump (LHD) vehicles and wheel loaders, whose articulated structures are similar to those of road rollers. Nayl *et al.* [18] proposed a sliding mode controller based on a novel continuous sliding surface and the nonlinear kinematic equations, being applied to the case of a LHD vehicle. They also analyzed the effect of kinematic parameters on model predictive controller (MPC) using a simulated LHD model in [19]. Alshaer *et al.* [20], [21] modeled the wheel loader as a multi-body mechanical system and applied the model to track the desired path with a fuzzy logic controller and a proportional integral derivative (PID) controller. Dou *et al.* [22] developed a novel relative navigation control law based on neural network and spatial geometric relationships for articulated underground vehicles. Nevertheless, it is noted that the above-mentioned vehicles have two front wheels while the road rollers generally have a rigid drum in the front. Quaglia *et al.* [23] developed a simplified dynamic model of a novel snake robot designed at Politecnico di Torino, which has the same system layout with a road roller. Unfortunately, due to its snake-like architecture in the motion phase, the tangential forces generated between ground and rollers depend on sideslip effect, differing from those of road rollers. As a result, these methods may not also be suitable for path tracking control of an articulated road roller.

Recently, several attempts have been made in path tracking control of a road roller. Yao *et al.* [24] discussed the steering kinematics of a road roller, and proposed a trajectory tracking method with disturbance-resistant and heading estimation. The impact of attitude feedback and control structure on the path following control of unmanned road rollers have been analyzed in [25] and [26] respectively. Chen *et al.* [27] proposed an active disturbance rejection control, featured with estimating and cancelling "total disturbance". Although these papers have proposed different control methods for the path tracking problem of road roller, they fail to take into account the control input saturation, which is limited by the mechanical saturation interval of vehicle. Furthermore, the existing studies only focus on ideal mathematical models or environments. To the authors' best knowledge, there are few studies considering sideslip effect and its compensation in path tracking control of a road roller, which has a serious influence on the compaction quality and efficiency of unmanned road roller.

In this paper, a path tracking control method of an articulated road roller with sideslip compensation is proposed. Firstly, the mathematical model is finalized in the presence of sideslip effect. Then, a path tracking control law based on proposed error dynamic equation and preview strategy is designed, and the control input is only the steering angle dynamic. To evaluate the control performance of the proposed method, a comparison with control laws containing sideslip compensation and non-compensation is performed through simulations and experiments. Finally, the simulation and experimental results demonstrate that the proposed method can ensure the articulated road roller lock into a desired path in bumpy environments, proving its effectiveness and feasibility.

The remainder of this paper is structured as follows. Section II describes the vehicle model with sideslip applied in the proposed control law, including kinematic model and dynamic model. In Section III, a path tracking control problem is established considering sideslip effect, which is based on designed preview controller. A series of numerical simulations under the MATLAB/Simulink is performed in Section IV to verify the effectiveness. Section V describes the experiments conducted to demonstrate the performance of the proposed method. Results of the experiments are further discussed in detail. Finally, the conclusions are stated in Section VI.

II. ARTICULATED ROAD ROLLER MODELING WITH SIDESLIP

The mathematical model, describing motion state of articulated road roller, has played an important role in solving path tracking problem. According to its function, the model can be divided into kinematic model and dynamic model. In order to obtain satisfactory control results, the kinematic and dynamic characteristics of articulated road roller have been considered simultaneously in this paper. However, due to the effect of suspension movements and frequent steering, sideslip is indispensable when the articulated road roller is working, especially in bumpy environments. Thus, the influence of sideslip has also been considered during vehicle modeling. In this section, the kinematic model and dynamic model of articulated road roller are established, and the corresponding derivation process is described.

A. KINEMATIC MODEL

The kinematic model of an articulated road roller can be simplified as two frames (front and rear) and an active revolute joint, as shown in Figure 1. In which OXY is the global Cartesian coordinate system, $P\,(x_P, y_P)$ is the midpoint of the front frame's roller axle, θ_P is the heading angle of the desired path with respect to the positive X axis, β is the sideslip angle

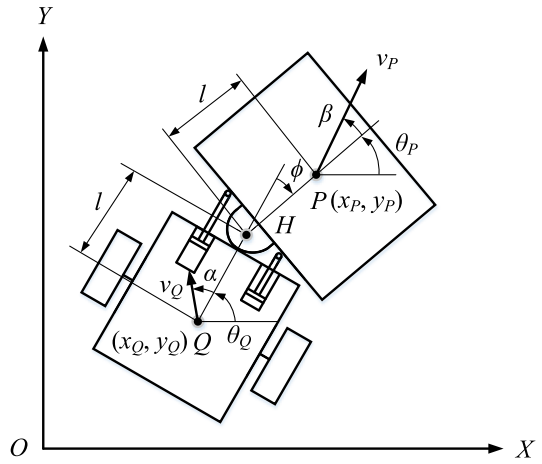

FIGURE 1. Kinematic model of the articulated road roller with sideslip.

of the front frame with respect to the positive perpendicular direction of roller axle, v_P is the forward velocity of the front frame, ϕ is the steering angle of the front frame with respect to the heading direction, $Q\left(x_Q, y_Q\right)$ is the midpoint of the rear frame's wheel axle, θ_Q is the desired heading angle of the rear frame with respect to the positive X axis, α is the sideslip angle of the rear frame with respect to the positive perpendicular direction of wheel axle, v_Q is the forward velocity of the rear frame, l is the distance from the junction point H to the midpoint of the roller axle and the wheel axle.

According to the depicted geometrical characteristics of the vehicle, the coordinate change of the midpoint P of front frame's roller axle can be derived as follows:

$$\begin{aligned} \dot{x}_P &= v_P \cos\left(\theta_P + \beta\right) \\ \dot{y}_P &= v_P \sin\left(\theta_P + \beta\right) \end{aligned} \tag{1}$$

Since two frames of road roller are articulated by the junction point H, their velocity constraints can be represented by the following expression:

$$\boldsymbol{v_P} + \dot{\theta}_P \times \boldsymbol{PH} = \boldsymbol{v_Q} + \dot{\theta}_Q \times \boldsymbol{QH} \tag{2}$$

where $\dot{\theta}_P$ and $\dot{\theta}_Q$ are the angular velocities of front and rear frames respectively.

Here, it can be observed that the forward velocities v_P and v_Q have the same change rule with respect to the velocity of junction point H. For the convenience of calculation, Equation (2) can be substituted into a vector decomposition formulation:

$$\begin{bmatrix} \cos\alpha & 0 \\ \sin\alpha & -l \end{bmatrix} \begin{bmatrix} v_Q \\ \dot{\theta}_Q \end{bmatrix} = \begin{bmatrix} \cos\phi & -\sin\phi \\ \sin\phi & \cos\phi \end{bmatrix} \times \begin{bmatrix} \cos\beta & 0 \\ \sin\beta & l \end{bmatrix} \begin{bmatrix} v_P \\ \dot{\theta}_P \end{bmatrix} \tag{3}$$

Additionally, it is quite evident from Figure 1 that there is a geometrical relationship given by:

$$\theta_Q = \theta_P + \phi \tag{4}$$

Substituting Equation (4) into Equation (3), the angular velocity $\dot{\theta}_P$ of the front frame is derived as follows:

$$\dot{\theta}_P = \frac{-v_P \sin\left(\phi + \beta - \alpha\right) - l\dot{\phi}\cos\alpha}{l\cos\alpha + l\cos\left(\phi - \alpha\right)} \tag{5}$$

On the basis of the equations above, the kinematic model of an articulated road roller with sideslip is proposed as shown in the following expression:

$$\begin{bmatrix} \dot{x}_P \\ \dot{y}_P \\ \dot{\theta}_P \\ \dot{\phi} \end{bmatrix} = \begin{bmatrix} \cos\left(\theta + \beta\right) & 0 \\ \sin\left(\theta + \beta\right) & 0 \\ \dfrac{-\sin\left(\phi + \beta - \alpha\right)}{L} & \dfrac{-l\cos\alpha}{L} \\ 0 & 1 \end{bmatrix} \begin{bmatrix} v_P \\ \dot{\phi} \end{bmatrix} \tag{6}$$

where $L = l\cos\alpha + l\cos\left(\phi - \alpha\right)$.

B. DYNAMIC MODEL

The dynamic model of an articulated road roller can be established by combining its force condition during operation with the kinematic model.

As depicted in Figure 1, the front frame is connected to the rear frame through an active revolute joint. The driving motion of road roller is motivated by the tractive force acting on the rear wheels, and the steering motion is driven by the steering torque acting on the junction point. In practical rolling compaction, the operating velocity of road roller is typically rather slow, which is lower than 5 km/h. Therefore, it is noted that the eccentric force caused by steering at high velocities, and the air resistance are neglected in this paper.

In vehicle-based coordinate system of front frame, its kinematic velocities can be described by the derivatives of vector $q^T = [x_P, y_P, \theta_P, \phi]$, as follows:

$$\begin{bmatrix} v_{Px} \\ v_{Py} \\ \dot{\theta}_P \end{bmatrix} = \begin{bmatrix} \cos\theta_P & \sin\theta_P & 0 & 0 \\ \sin\theta_P & -\cos\theta_P & 0 & 0 \\ 0 & 0 & 1 & 0 \end{bmatrix} \begin{bmatrix} \dot{x}_P \\ \dot{y}_P \\ \dot{\theta}_P \\ \dot{\phi} \end{bmatrix} \tag{7}$$

where v_{Px} and v_{Py} are the longitudinal and lateral velocities of the front frame respectively.

Similarly, the kinematic velocities of rear frame are given by:

$$\begin{bmatrix} v_{Qx} \\ v_{Qy} \\ \dot{\theta}_Q \end{bmatrix} = \begin{bmatrix} \cos\theta_Q & \sin\theta_Q & 0 & 0 \\ \sin\theta_Q & -\cos\theta_Q & 0 & 0 \\ 0 & 0 & 1 & 0 \end{bmatrix} \begin{bmatrix} \dot{x}_Q \\ \dot{y}_Q \\ \dot{\theta}_Q \\ \dot{\phi} \end{bmatrix} \tag{8}$$

where v_{Qx} and v_{Qy} are the longitudinal and lateral velocities of the rear frame respectively.

By using the geometric relationship:

$$\begin{aligned} x_Q &= x_P - l\left(\cos\theta_P + \cos\theta_Q\right) \\ y_Q &= y_P - l\left(\sin\theta_P + \sin\theta_Q\right) \end{aligned} \tag{9}$$

the Equation (8) can be rewritten as:

$$\begin{bmatrix} v_{Qx} \\ v_{Qy} \\ \dot{\theta}_Q \end{bmatrix} = \begin{bmatrix} \cos\theta_Q & \sin\theta_Q & -l\sin\phi & 0 \\ \sin\theta_Q & -\cos\theta_Q & l\left(1 + \cos\phi\right) & l \\ 0 & 0 & 1 & 1 \end{bmatrix} \begin{bmatrix} \dot{x}_P \\ \dot{y}_P \\ \dot{\theta}_P \\ \dot{\phi} \end{bmatrix} \tag{10}$$

Combining Equations (4), (6), (7) and (10), the kinematic velocities of road roller can be indicated by the generalized velocity vector $V^T = \left[v_P, \dot{\theta}_P\right]$, as shown in the following expression:

$$\begin{bmatrix} v_{Px} \\ v_{Py} \\ \dot{\theta}_P \\ v_{Qx} \\ v_{Qy} \\ \dot{\theta}_Q \end{bmatrix} = \begin{bmatrix} \cos\theta_P & \sin\theta_P & 0 & 0 \\ \sin\theta_P & -\cos\theta_P & 0 & 0 \\ 0 & 0 & 1 & 0 \\ \cos(\theta_P+\phi) & \sin(\theta_P+\phi) & -l\sin\phi & 0 \\ \sin(\theta_P+\phi) & -\cos(\theta_P+\phi) & l(1+\cos\phi) & l \\ 0 & 0 & 1 & 1 \end{bmatrix} \times \begin{bmatrix} \cos(\theta_P+\beta) & 0 \\ \sin(\theta_P+\beta) & 0 \\ 0 & 1 \\ \frac{-\sin(\phi+\beta-\alpha)}{l\cos\alpha} & -\frac{\cos\alpha+\cos(\phi-\alpha)}{\cos\alpha} \end{bmatrix} \begin{bmatrix} v_P \\ \dot{\theta}_P \end{bmatrix} \quad (11)$$

From the above equation, the matrix J transforming generalized velocities to kinematic velocities is obtained as:

$$J = \begin{bmatrix} \cos\beta & 0 \\ -\sin\beta & 0 \\ 0 & 1 \\ \cos(\phi-\beta) & -l\sin\phi \\ a & \frac{-l\sin\phi\sin\alpha}{\cos\alpha} \\ b & \frac{-\cos(\phi-\alpha)}{\cos\alpha} \end{bmatrix} \quad (12)$$

where

$$a = \frac{\sin(\alpha-\beta)\cos\phi - \sin\beta\cos(\phi-\alpha)}{\cos\alpha},$$
$$b = \frac{\sin(\phi+\beta-\alpha)}{\cos\alpha}.$$

According to Kane's dynamical equation [28], the dynamic model of an articulated road roller submitted to holonomic and non-holonomic constraints is defined as follows:

$$\begin{aligned} N(q) &= J^T M J \\ F(q,V) &= -J^T\left(M\dot{J} + WMJ\right)V \\ N(q)\dot{V} &= F(q,V) + J^T w \end{aligned} \quad (13)$$

where $N(q)$ is the inertia matrix of road roller, M is the extended mass matrix of road roller, $F(q,V)$ is the force vector representing Coriolis and centripetal forces, W is the extended angular velocity matrix of road roller, w is the vector describing the active forces and torques of system.

From Equations (12) and (13), the inertia matrix $N(q)$ is calculated as

$$N(q) = \begin{bmatrix} n_{11} & n_{12} \\ n_{21} & n_{22} \end{bmatrix} \quad (14)$$

where

$$n_{11} = m_P + m_Q\cos^2(\phi-\beta) + m_Q a^2 + \frac{j_Q b^2}{l^2},$$
$$n_{12} = n_{21} = -m_Q l\sin\phi\cos(\phi-\beta) - \frac{m_Q a l\sin\phi\sin\alpha}{\cos\alpha} + \frac{j_Q b\cos(\phi-\alpha)}{l\cos\alpha},$$
$$n_{22} = j_P + m_Q l^2\sin^2\phi + \frac{m_Q l^2\sin^2\phi\sin^2\alpha}{\cos^2\alpha} + \frac{j_Q\cos(\phi-\alpha)}{\cos^2\alpha}.$$

In the above equations, it is noted that m_P and m_Q are the inertia mass of front and rear frames respectively, and the j_P and j_Q are the inertia torque of front and rear frames correspondingly.

Furthermore, the force vector $F(q,V)$ is obtained by using Equation (13), as follows:

$$F(q,V) = \begin{bmatrix} f_{11} & f_{12} \\ f_{21} & f_{22} \end{bmatrix} \begin{bmatrix} v_P \\ \dot{\theta}_P \end{bmatrix} \quad (15)$$

where

$$f_{11} = m_Q\dot{\phi}\left[\sin(\phi-\beta)\cos(\phi-\beta) - ac\right] - \frac{j_Q\dot{\phi}bd}{l^2},$$
$$f_{12} = m_Q l\dot{\phi}\left[\frac{\cos(\phi-\alpha)\cos(\phi-\beta) + a\sin(\phi+\alpha)}{\cos\alpha}\right] + m_Q l\left[a\sin\phi - \frac{\sin\phi\sin\alpha\cos(\phi-\beta)}{\cos\alpha}\right] + \frac{j_Q\dot{\phi}b\sin(\phi-\alpha)}{l\cos\alpha},$$
$$f_{21} = m_Q l\dot{\phi}\left[\frac{\sin\phi\sin\alpha\cos(\phi-\beta) + c\sin\phi\sin\alpha}{\cos\alpha}\right] - m_Q l\dot{\phi}\left[\sin\phi\sin(\phi-\beta) + a\sin\phi\right] + m_Q l\left[\frac{\sin\phi\sin\alpha\cos(\phi-\beta)}{\cos\alpha} - a\sin\phi\right] - \frac{j_Q\dot{\phi}d\cos(\phi-\alpha)}{l\cos\alpha},$$
$$f_{22} = -m_Q l^2\dot{\phi}\left[\frac{\sin\phi\cos(\phi-\alpha)}{\cos\alpha} + \frac{\sin\phi\sin\alpha\sin(\phi+\alpha)}{\cos^2\alpha}\right] + \frac{j_Q\dot{\phi}\sin(\phi-\alpha)\cos(\phi-\alpha)}{\cos^2\alpha},$$
$$c = \frac{\sin\beta\sin(\phi-\alpha) - \sin(\alpha-\beta)\sin\phi}{\cos\alpha},$$
$$d = \frac{\cos(\phi+\beta-\alpha)}{\cos\alpha}.$$

In addition, the active force and torque of system can be described by the vector $w^T = \left[f_Q, f_H\right]$. Therefore, the generalized forces τ are expressed as:

$$\tau = J^T w = T\begin{bmatrix} f_Q \\ f_H \end{bmatrix} \quad (16)$$

where f_Q is the tractive force acting on the rear wheels, namely the resultant force of driving force and friction, f_H is the steering torque acting on the junction point, and T is the transformation matrix given by:

$$T = \begin{bmatrix} \cos(\phi-\beta) & b/l \\ -l\sin\phi & 1+\cos(\phi-\alpha)/\cos\alpha \end{bmatrix} \quad (17)$$

Based on the above contents, the dynamic model of an articulated road roller with sideslip is finally proposed as follows:

$$N(q)\begin{bmatrix} \dot{v}_P \\ \ddot{\theta}_P \end{bmatrix} = F(q,V) + T\begin{bmatrix} f_Q \\ f_H \end{bmatrix} \quad (18)$$

III. PATH TRACKING CONTROL

To complete the rolling of the designated area, articulated road rollers are generally driven to move along the predetermined paths in actual construction. Thus, the aim of path tracking control is to make an articulated road roller lock into a desired path in bumpy environments. In this section, a mathematical error dynamic equation is proposed, and a state-feedback control law is designed to achieve the control purpose.

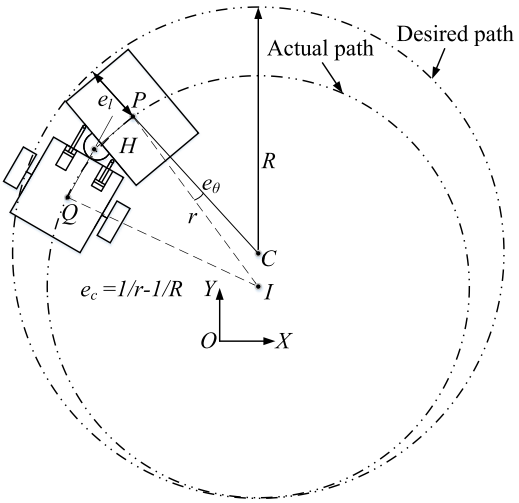

FIGURE 2. Path tracking control problem.

A. ERROR DYNAMIC EQUATION

Regarding the midpoint P of front frame's roller axle as the navigation point, the path tracking control problem can be depicted in Figure 2, where e_l is the displacement error, e_θ is the heading error, e_c is the curvature error, r is the turning radius of road roller, R is the curvature radius of desired path.

As mentioned above, the path tracking errors between the actual and the desired path are represented by the displacement error e_l, the heading error e_θ and the curvature error e_c. Here, it is worth pointing out that if the desired path is a straight line, the curvature error e_c will be zero.

Then, it is noted that if the navigation point P is rotating $\Delta\theta$ clockwise around the instantaneous center I to the next position P', path tracking errors will also change accordingly, as shown in Figure 3.

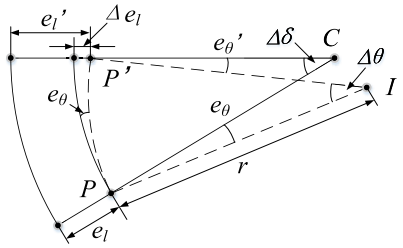

FIGURE 3. Dynamics of the path tracking errors.

Considering that $\Delta\theta$ and $\Delta\delta$ are very small, and R is far greater than e_l in actual path tracking control. The following geometrical relationships can be obtained from Figure 3:

$$\begin{aligned} \Delta e_l &= (r\Delta\theta)\, e_\theta \\ \Delta e_\theta &= \Delta\theta - \Delta\delta \\ R\Delta\delta &\approx r\Delta\theta \\ e_c &= \frac{1}{r} - \frac{1}{R} \end{aligned} \tag{19}$$

According to the first equality of Equation (19), the displacement error dynamic is proposed as:

$$\dot{e}_l = \frac{\Delta e_l}{\Delta t} = v_P e_\theta \tag{20}$$

where $v_P = r\Delta\theta \big/ \Delta t$

Combining the rest three equalities of Equation (19),the heading error dynamic is derived as follows:

$$\begin{aligned} \dot{e}_\theta &= \frac{\Delta e_\theta}{\Delta t} = \dot{\theta}_P \left(1 - \frac{r}{R}\right) \\ &= \dot{\theta}_P r \times e_c = v_P e_c \end{aligned} \tag{21}$$

From Equation (5), it is easily verified that the reciprocal of r can be calculated as:

$$\frac{1}{r} = \frac{\dot{\theta}_P}{v_P} = \frac{-v_P \sin(\phi + \beta - \alpha) - l\dot{\phi}\cos\alpha}{v_P\left[l\cos\alpha + l\cos(\phi - \alpha)\right]} \tag{22}$$

In order to calculate conveniently, the assumption has been made that the forward velocity v_P, sideslip angles β and α, the curvature radius of desired path R are all constant. What's more, it is noticed that ϕ, β and α are all very small under normal working conditions. Hence, their cosine functions can be approximately equal to 1, and their sine functions can be approximately equal to the angles themselves in radians.

From the above equation, the curvature error dynamic is yielded as follows:

$$\dot{e}_c = -\frac{\dot{\phi}}{4l}\left[2 + (\phi + \beta - \alpha)(\phi - \alpha)\right] \tag{23}$$

Finally, the linear error dynamic equation of an articulated road roller with sideslip is described as:

$$\begin{bmatrix} \dot{e}_l \\ \dot{e}_\theta \\ \dot{e}_c \end{bmatrix} = \begin{bmatrix} 0 & v_P & 0 \\ 0 & 0 & v_P \\ 0 & 0 & 0 \end{bmatrix} \begin{bmatrix} e_l \\ e_\theta \\ e_c \end{bmatrix} + \begin{bmatrix} 0 \\ 0 \\ -\dfrac{\gamma}{4l} \end{bmatrix} \dot{\phi} \tag{24}$$

where $\gamma = 2 + (\phi + \beta - \alpha)(\phi - \alpha)$.

B. DESIGN OF CONTROL LAW

From the mathematical point of view, the aim of path tracking control is to make the displacement error e_l, the heading error e_θ and the curvature error e_c converge to zero over time. Analyzing the linear error dynamic equation, it is found that the steering angle dynamic $\dot{\phi}$ can be selected as control input to achieve the path tracking of a road roller.

Preview control is a widely used approach in vehicle path tracking control, with the advantages of fast response and high convergence performance [29]–[32]. The basic idea of

this control law is tantamount to anticipate the path ahead and adjust the steering angle based on knowledge of the vehicle dynamics, compensating for the path tracking errors. Here, a path tracking control law based on proposed preview strategy is being designed.

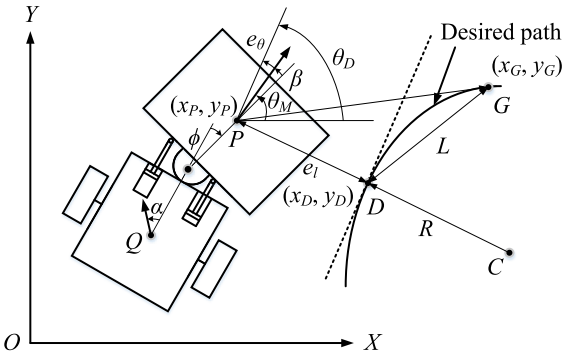

FIGURE 4. Schematic of the path tracking control law based on proposed preview strategy.

As shown in Figure 4, where θ_D is the desired heading angle, θ_M is the current heading angle, $G(x_G, y_G)$ is the target point on the desired path, $D(x_D, y_D)$ is the desired point, and L is the preview distance. The controller makes an appropriate steering action based on the displacement error e_l, the heading error e_θ and the front sideslip angle β at the corresponding velocity. In terms of the controller, its purpose is to eliminate the path tracking errors between the actual path and the desired path. To facilitate understanding, an improved heading error E_θ is proposed as:

$$E_\theta = e_\theta + \beta \tag{25}$$

Consequently, the path tracking control law is designed as follows:

$$\dot{\phi} = k\left(\arctan\left(\frac{e_l}{L}\right) + E_\theta\right) \tag{26}$$

where k is the adjustment factor.

Moreover, it is important to note that the target point and preview distance are obtained according to the work by Liu and Duan [33]. The current heading and steering angles can be measured by a sensor system in practice. And, other unknown state variables can be calculated as:

$$\begin{aligned} e_l &= (x_D - x_P)\sin\theta_D + (y_P - y_D)\cos\theta_D \\ E_\theta &= \theta_D - \theta_M + \beta \\ L &= \sqrt{(x_G - x_D)^2 + (y_G - y_D)^2} \end{aligned} \tag{27}$$

Due to the slow response of steering system powered by hydraulic cylinders, the current heading angle θ_M is considered as a constant in one sample period ΔT. Therefore, the estimation of front sideslip angle β can be calculated as:

$$\beta = \psi - \theta_M \tag{28}$$

where ψ is the instantaneous heading angle, given by:

$$\psi = \arctan\left(\frac{y_P[n] - y_P[n-1]}{x_P[n] - x_P[n-1]}\right) \tag{29}$$

Similarly, the rear sideslip angle α can also be estimated, depending on the midpoint Q of rear frame's wheel axle.

The overall block diagram of the proposed path tracking control is depicted in Figure 5.

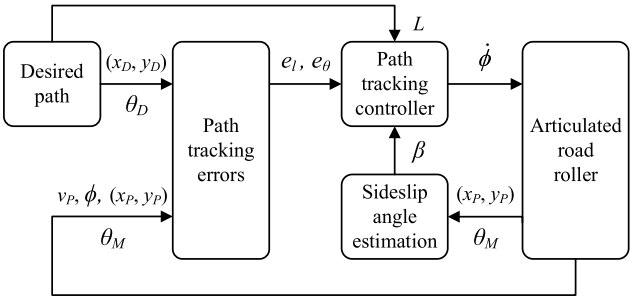

FIGURE 5. Overall block diagram of the proposed path tracking control.

IV. SIMULATIONS

In this section, the effectiveness and feasibility of the proposed path tracking control law will be verified by numerical simulation, which is conducted via MATLAB/Simulink. In the simulation model, it is assumed that all state variables have been measured directly or calculated. Hence, the positioning system and the sensing system are not included in the simulation. The action of the control law is the steering angle dynamic which constraints on the states of path tracking errors. There is no doubt that tracking a curved path is more difficult. According to the construction requirements, it is noted that the compaction path is mainly consisted of straight-line and circular path in reality [24]. Hence, the desired path is expected to be a circle, which can test the lateral and steering maneuvers well due to its curvature radius.

TABLE 1. Simulation parameters for the path tracking control.

Symbol	Description	Value
m_P	Inertia mass of front frame (kg)	17100
m_Q	Inertia mass of rear frame (kg)	9600
j_P	Inertia torques of front frame ($\mathrm{kg \cdot m^2}$)	55231
j_Q	Inertia torques of rear frame ($\mathrm{kg \cdot m^2}$)	43606
l	Length of PH and QH (m)	1.63
e_θ	Initial heading error (rad)	-0.0635
S	Initial position of road roller (m)	$(0,6)$
v_P	Forward velocity of road roller (km/h)	2.7
k	Adjustment factor	1.28
L	Preview distance (m)	3.5
β	Sideslip angle of front frame (rad)	0.105
α	Sideslip angle of rear frame (rad)	0.052
ϕ	Steering angle (rad)	$[-0.611, 0.611]$
$\dot{\phi}$	Steering angle velocity (rad/s)	$[-0.2, 0.2]$

As shown in Table 1, the following vehicle's parameters have been obtained referring to the manual of an SSR260 articulated road roller: the inertia mass of front and

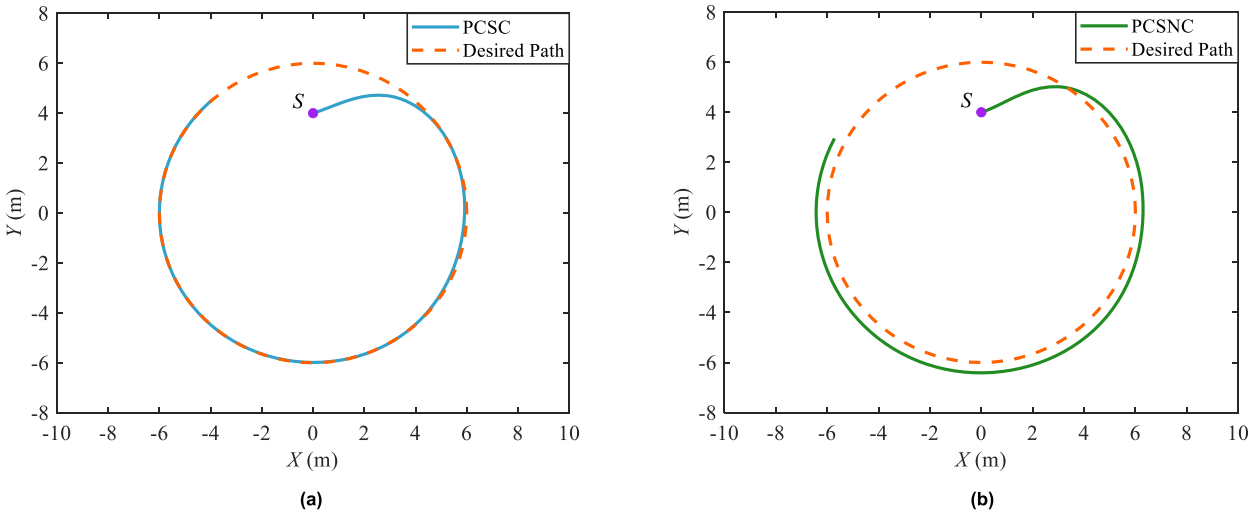

FIGURE 6. Simulation results of road roller tracking a circular path in the existence of sideslip using preview controller with the sideslip compensation and non-compensation. (a) PCSC; (b) PCSNC.

rear frames is respectively given as $m_P = 17100$ kg and $m_Q = 9600$ kg, the inertia torques of front and rear frames are correspondingly calculated as $j_P = 55231$ kg $\cdot$ m^2 and $j_Q = 43606$ kg $\cdot$ m^2, the length of PH and QH is 1.63 m.

Besides, initial states associated with steering angle, heading angle, and position coordinates are supposed as 0 rad, -0.0635 rad, and $(0, 6)$. The center of the circular path is at $(0, 0)$, whose radius is 6 m. The velocity of road roller is typically set as $v_P = 2.7$ km/h.The adjustment factor used in the simulation is determined by tuning in experiments as $k = 1.28$. Similarly, the preview distance is set as $L = 3.5$ m. For the convenience of simulation, the sideslip angles of front and rear frames are assumed as $\beta = 0.105$ rad and $\alpha = 0.052$ rad. Considering the driving stability and safety under various working conditions, the steering angle ϕ is limited to $[-0.611, 0.611]$ rad, and its corresponding dynamic $\dot{\phi}$ is limited to $[-0.2, 0.2]$ rad/s, by the mechanical saturation interval of vehicle.

Figure 6 depicts that the simulation results of articulated road roller tracking a circular path with sideslip effect in Cartesian plane, where the solid blue line represents the actual path based on the PCSC, the solid green line stands for the actual path based on the preview controller with sideslip non-compensation (PCSNC), and the dotted red line plots the desired one. From the simulation results, it can be observed that PCSC performs better which converges to the desired path closer. Due to the existence of sideslip, the actual path based on PCSNC keeps a certain distance away from the desired path all the time. In contrast, the method using PCSC can navigate the road roller to track the desired path asymptotically. As a consequent, it reveals that the proposed method can provide a rather satisfactory performance.

Moreover, the time-histories of road roller responses for PCSC and PCSNC are depicted in Figure 7. It can be found that the road roller adjusts sharply at the beginning, which is attributable to the initial errors. After about 15 s, the adjustment becomes smooth gradually. However, it can be observed that displacement error and curvature error with PCSC are close and approaching to zero as time goes by. While, corresponding errors cannot converge to zero without sideslip compensation. Compared with the PCSNC, the proposed PCSC algorithm can achieve higher accuracy of path tracking and stronger robustness simultaneously. It is worth mentioning that the PCSC-based and PCSNC-based improved heading errors both converge to zero after 35 s. This is due to the fact that the sideslip effect primarily affects displacement errors rather than the errors between the direction of actual velocity and the desired heading angle.

In addition, Figure 7(d) indicates the time responses of steering angle, which displays that the related control input can satisfy the constraints predefined by the mechanical saturation interval of vehicle during the adjustment process.

Above all, the proposed PCSC method can achieve exact path tracking in the existence of sideslip, confirming its effectiveness and feasibility. Besides this, the PCSC can not only improve the control accuracy, but also increase the convergence rate, which is superior to the PCSNC method.

V. EXPERIMENTS

To validate the stability and reconfigurability of PCSC in practical application, automatic compaction experiments were performed on a road roller at the construction site of Chang-he Dam hydroelectric power station, which is located in Sichuan Province, China. Figure 8 shows the automatic compaction experiment on the main rockfill, and the maximum diameter of rocks is about 300 mm. Large rocks and inclines enhance the sideslip effect. There is no doubt that path tracking control in bumpy environments is more difficult than on a flat road.

A. SYSTEM SETUP

A SSR260 smooth road roller is modified with various devices to achieve the path tracking control in the experiment, as shown in Figure 9. A SPS855 Trimble GNSS receiver is

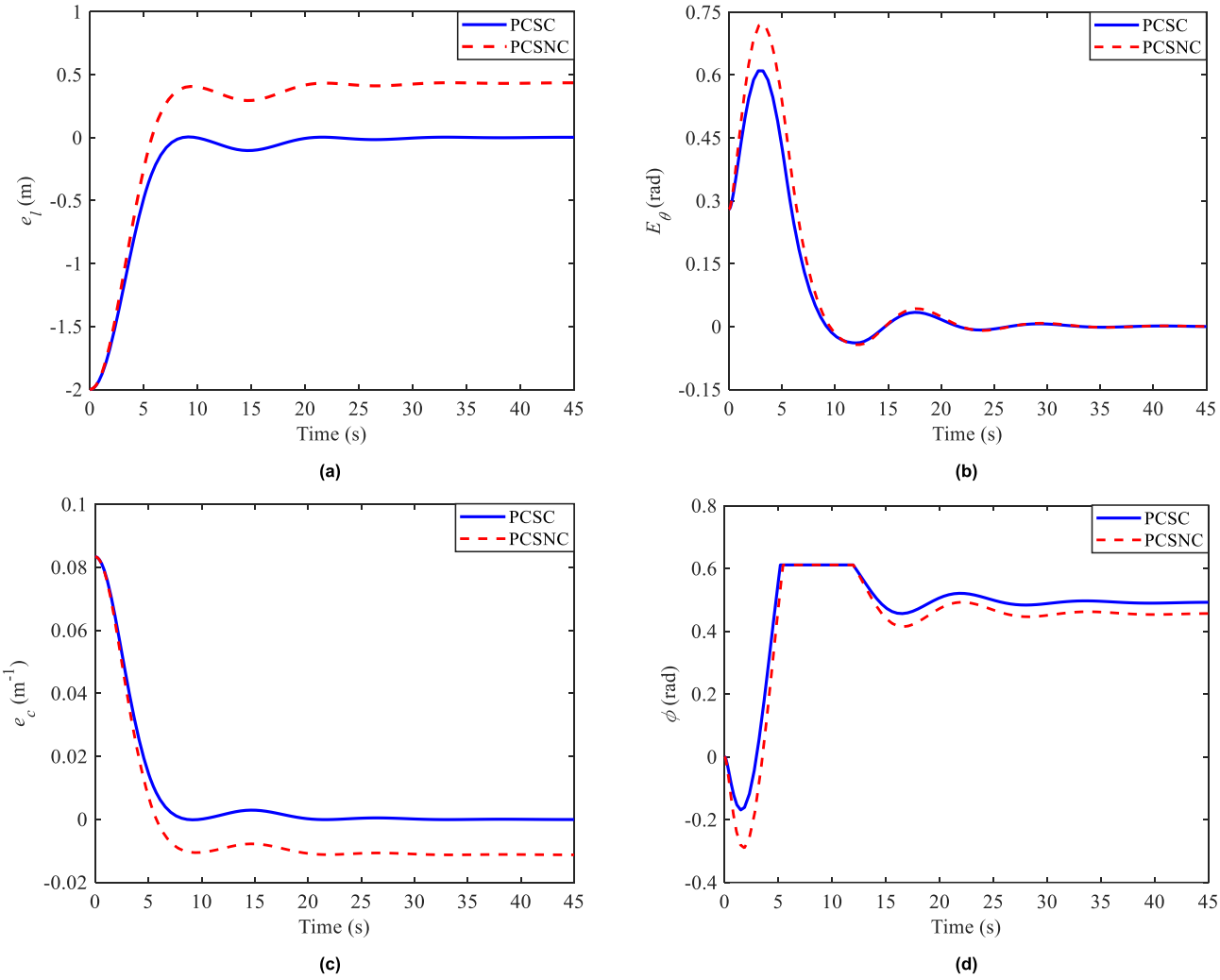

FIGURE 7. Simulation comparison of time responses for PCSC and PCSNC in tracking a circular path with sideslip effect. (a) displacement error; (b) improved heading error; (c) curvature error; (d) steering angle.

FIGURE 8. Automatic compaction experiment on the main rockfill.

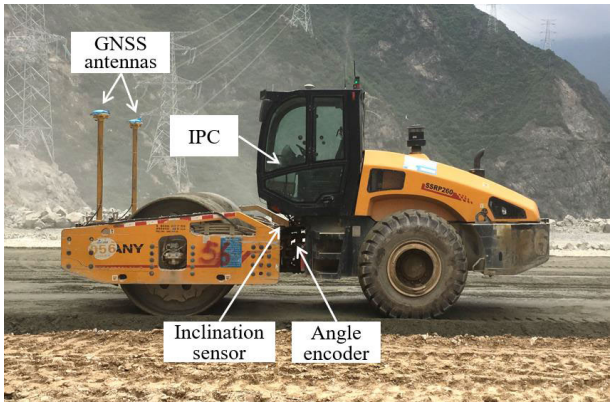

FIGURE 9. A modified SSR260 road roller used in the experiment.

mounted in the driver's cab to measure the position coordinates of frame, whose horizontal and vertical accuracy is as high as 8 mm and 15 mm respectively when working in Real Time Kinematic (RTK) mode. The forward velocity can be indicated by the output of NMEA protocol in real time, and the coordinates of desired point are then derived from the

FIGURE 10. Experimental devices equipped on the SSR260 road roller. (a) SPS855 and SPS555 Trimble GNSS receivers; (b) base station; (c) multi-turn angle encoder; (d) inclination sensor; (e) industrial personal computer.

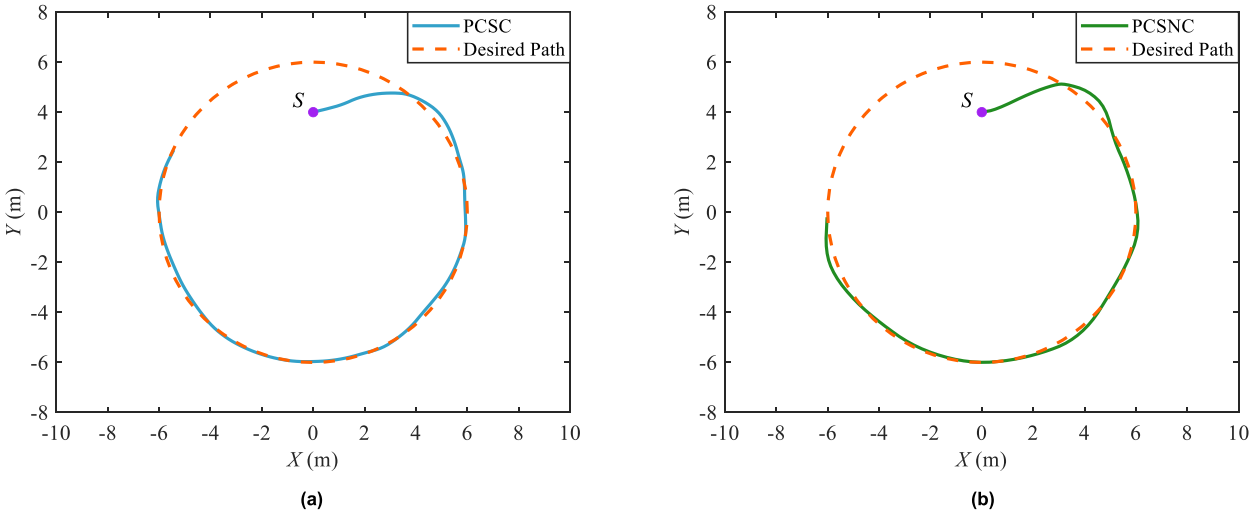

FIGURE 11. Experimental results of road roller tracking a circular path in the existence of sideslip using preview controller with the sideslip compensation and non-compensation. (a) PCSC; (b) PCSNC.

positioning data by coordinate transformation. A SPS555H Trimble heading receiver is applied to obtain the real-time heading of front frame by combining the positioning data received from positioning and heading antennas, with the accuracy of 0.09 degrees. As shown in Figure 10(b), another SPS855 Trimble GNSS receiver is configured as the base station to correct the positioning data. With their own excellent computing and filtering performance, the Trimble GNSS receivers are able to ensure the stability of the measurement accuracy. Then, path tracking errors and sideslip angle are calculated by the relative position and heading data.

Furthermore, a multi-turn angle encoder is placed in the revolute joint to measure the real-time steering angle, connecting via CANopen and offering up to 0.1 degrees accuracy, as shown in Figure 10(c). To compensate the positioning error caused by the variation of front frame in terms of pitch and roll angles, a two-dimensional inclination sensor is mounted on the front frame, with the accuracy of 0.1 degrees and the measurement range of ± 45 degrees, as shown in Figure 10(d).

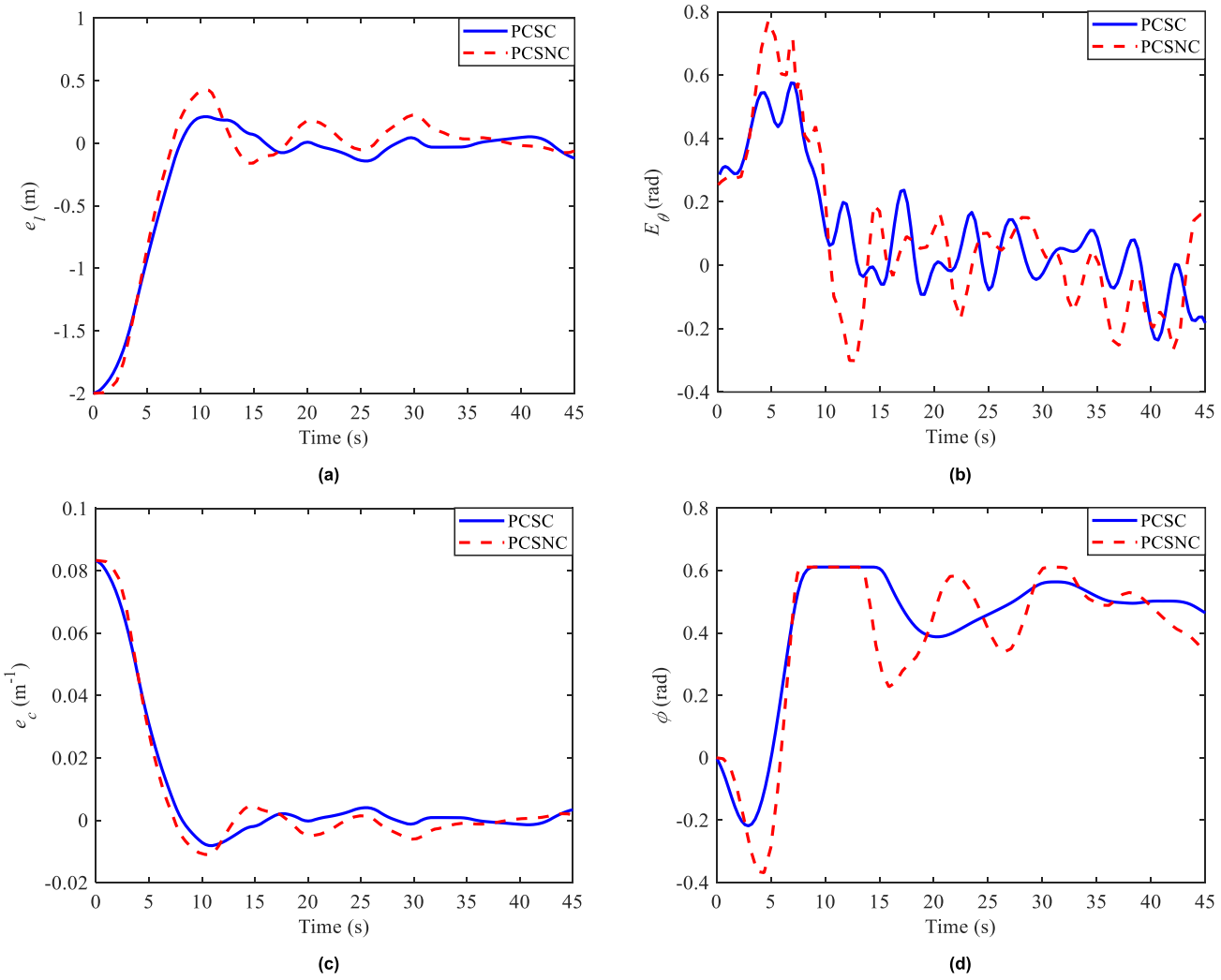

FIGURE 12. Experimental comparison of time responses for PCSC and PCSNC in tracking a circular path with sideslip effect. (a) displacement error; (b) improved heading error; (c) curvature error; (d) steering angle.

In addition, an industrial personal computer (IPC) is utilized to execute the path tracing methods, and record the experimental results. For the purpose of satisfying the system requirements for real-time, a control area network (CAN) is also introduced to transmit the control and status signals of vehicle.

B. RESULTS AND DISCUSSION

In order to ensure a fair and valid comparison, the initial values of displacement error, heading error, and steering angle in the experiments are identical with those of the simulation models. As shown in Figure 11, the mentioned automatic compaction experiments were performed on the same desired circular path, which contributes to analyzing the control accuracy of the path tracking methods with and without sideslip compensation. Then, Figure 12(a)∼(d) correspondingly illustrates the comparisons of displacement error e_l, improved heading error E_θ, curvature error e_c and steering angle ϕ between these two different path tracking controller, namely PCSC and PCSNC.

From Figure 11, it can be seen that the method based on PCSC converges to the desired circular path closer, which is quite similar to the simulation results. Besides this, the actual path based on PCSC is much rounder and smoother in shape than other benchmark method, showing that its stability is better. Moreover, the position delay of vehicle in the non-compensation condition is more obvious than that in the compensation condition. The reason is primarily due to the increase in adjustment time under the same circumstances of forward velocity.

Figure 12 depicts that displacement error, improved heading error and curvature error with PCSC of experiments tend to be zero with increase in time, even if they are given initial conditions. Meanwhile, the steering angle and related control input were not also saturated. In other words, the effectiveness and feasibility of the proposed path tracking control law are confirmed by both simulations and experiments, as well as

the established models considering sideslip angles. However, compared with the simulation results, the fluctuation of time responses for PCSC and PCSNC both are much larger, owing to the fact that the sideslip angles were constantly changing. For the same reason, the frequency and amplitude of adjustment also become larger accordingly.

Additionally, it is noted that the time responses of experiments are delayed in comparison with simulation results. This is explained by the fact that the response delay of steering cylinders powered by hydraulic system is not considered in the simulation. Fortunately, there is no any significant effect on the control performance.

In summary, according to the experimental results, it demonstrates once again that the proposed PCSC controller is an effective approach for tracking performance to reach a high accuracy, whose superiority is also verified.

VI. CONCLUSION

In this paper, a novel and effective method based on PCSC and the established models with sideslip for path tracking control of articulated road roller is proposed. Kinematic and dynamic models accounting for sideslip effect are firstly established. Then, a preview controller is designed to eliminate the path tracking errors in automatic compaction while compensating the sideslip effect. Next, the control performance of PCSC is evaluated by the numerical simulations and automatic compaction experiments. The simulation and experimental results show that an articulated road roller given an initial condition can be navigated to track a desired path in the existence of sideslip, with the proposed control law. What's more, the method based on PCSC not only improves the control accuracy, but also increases the convergence rate, which may have implications and wide application in the path tracking control of unmanned road roller.

ACKNOWLEDGMENT

The authors would like to thank editor and reviewers for their valuable comments and suggestions, which helped them improve the manuscript.

REFERENCES

[1] Q. Zhang, T. Liu, Z. Zhang, Z. Huangfu, Q. Li, and Z. An, "Unmanned rolling compaction system for rockfill materials," *Autom. Construct.*, vol. 100, pp. 103–117, Apr. 2019.

[2] D. Liu, M. Lin, and S. Li, "Real-time quality monitoring and control of highway compaction," *Autom. Construct.*, vol. 62, pp. 114–123, Feb. 2016.

[3] P. Shen and S. Lin, "Mathematic modeling and chaotic identification for practice construction in vibratory compacting," *J. Vibrat. Eng. Technol.*, vol. 6, no. 1, pp. 1–13, Jun. 2018.

[4] B. Zhang, C. Zong, G. Chen, and B. Zhang, "Electrical vehicle path tracking based model predictive control with a Laguerre function and exponential weight," *IEEE Access*, vol. 7, pp. 17082–17097, 2019.

[5] L. Liu, D. Wang, Z. Peng, T. Li, and C. L. P. Chen, "Cooperative path following ring-networked under-actuated autonomous surface vehicles: Algorithms and experimental results," *IEEE Trans. Cybern.*, vol. 50, no. 4, pp. 1519–1529, Apr. 2020.

[6] G. Bai, L. Liu, Y. Meng, W. Luo, Q. Gu, and J. Wang, "Path tracking of wheeled mobile robots based on dynamic prediction model," *IEEE Access*, vol. 7, pp. 39690–39701, 2019.

[7] G. Carabin, A. Gasparetto, F. Mazzetto, and R. Vidoni, "Design, implementation and validation of a stability model for articulated autonomous robotic systems," *Robot. Auto. Syst.*, vol. 83, pp. 158–168, Sep. 2016.

[8] S. Liu, Z. Hou, T. Tian, Z. Deng, and L. Guo, "Path tracking control of a self-driving wheel excavator via an enhanced data-driven model-free adaptive control approach," *IET Control Theory Appl.*, vol. 14, no. 2, pp. 220–232, Jan. 2020.

[9] Y. Zhang, A. Khajepour, E. Hashemi, Y. Qin, and Y. Huang, "Reconfigurable model predictive control for articulated vehicle stability with experimental validation," *IEEE Trans. Transport. Electrific.*, vol. 6, no. 1, pp. 308–317, Mar. 2020.

[10] M. Yue, X. Wu, L. Guo, and J. Gao, "Quintic polynomial-based obstacle avoidance trajectory planning and tracking control framework for tractor-trailer system," *Int. J. Control, Autom. Syst.*, vol. 17, no. 10, pp. 2634–2646, Jul. 2019.

[11] A. K. Khalaji, "PID-based target tracking control of a tractor-trailer mobile robot," *Proc. Inst. Mech. Eng., Part C, J. Mech. Eng. Sci.*, vol. 233, no. 13, pp. 4776–4787, Jul. 2019.

[12] N. T. Binh, N. A. Tung, D. P. Nam, and N. H. Quang, "An adaptive backstepping trajectory tracking control of a tractor trailer wheeled mobile robot," *Int. J. Control, Autom. Syst.*, vol. 17, no. 2, pp. 465–473, Jan. 2019.

[13] J. Shao, X. Zhao, J. Yang, W. Zhang, and Y. Kang, "Reinforcement learning algorithm for path following control of articulated vehicle," *Trans. Chin. Soc. Agricult. Mach.*, vol. 48, no. 3, pp. 376–382, Mar. 2017.

[14] M. Yue, X. Hou, R. Gao, and J. Chen, "Trajectory tracking control for tractor-trailer vehicles: A coordinated control approach," *Nonlinear Dyn.*, vol. 91, no. 2, pp. 1061–1074, Jan. 2018.

[15] A. K. Khalaji and M. Jalalnezhad, "Control of a tractor-trailer robot subjected to wheel slip," *Proc. Inst. Mech. Eng. Part K, J. Multi-Body Dyn.*, vol. 233, no. 4, pp. 956–967, 2019.

[16] E. Kayacan, W. Saeys, H. Ramon, C. Belta, and J. M. Peschel, "Experimental validation of linear and nonlinear MPC on an articulated unmanned ground vehicle," *IEEE/ASME Trans. Mechatronics*, vol. 23, no. 5, pp. 2023–2030, Oct. 2018.

[17] S. Zhou, H. Zhao, W. Chen, Z. Miao, Z. Liu, H. Wang, and Y.-H. Liu, "Robust path following of the tractor-trailers system in GPS-denied environments," *IEEE Robot. Autom. Lett.*, vol. 5, no. 2, pp. 500–507, Apr. 2020.

[18] T. Nayl, G. Nikolakopoulos, T. Gustafsson, D. Kominiak, and R. Nyberg, "Design and experimental evaluation of a novel sliding mode controller for an articulated vehicle," *Robot. Auto. Syst.*, vol. 103, pp. 213–221, May 2018.

[19] T. Nayl, G. Nikolakopoulos, and T. Gustafsson, "Effect of kinematic parameters on MPC based on-line motion planning for an articulated vehicle," *Robot. Auto. Syst.*, vol. 70, pp. 16–24, Aug. 2015.

[20] B. J. Alshaer, T. T. Darabseh, and A. Q. Momani, "Modelling and control of an autonomous articulated mining vehicle navigating a predefined path," *Int. J. Heavy Vehicle Syst.*, vol. 21, no. 2, pp. 152–168, 2014.

[21] B. J. Alshaer, T. T. Darabseh, and M. A. Alhanouti, "Path planning, modeling and simulation of an autonomous articulated heavy construction machine performing a loading cycle," *Appl. Math. Model.*, vol. 37, no. 7, pp. 5315–5325, Apr. 2013.

[22] F. Dou, Y. Meng, L. Liu, and Q. Gu, "A novel relative navigation control strategy based on relation space method for autonomous underground articulated vehicles," *J. Control Sci. Eng.*, vol. 2016, pp. 1–12, Oct. 2016.

[23] G. Quaglia, P. Cavallone, and B. Lenzo, "On the dynamic analysis of a novel snake robot: Preliminary results," in *Advances in Italian Mechanism Science* (Mechanisms and Machine Science), vol. 68, G. Carbone and A. Gasparetto, Eds. Cham, Switzerland: Springer, 2019, pp. 275–285.

[24] D. Yao, H. Xie, W. Qiang, Y. Liu, and S. Xiong, "Accurate trajectory tracking with disturbance-resistant and heading estimation method for self-driving vibratory roller," *IFAC-PapersOnLine*, vol. 51, no. 31, pp. 754–758, 2018.

[25] W. Zhan, H. Xie, Q. Xu, K. Song, and W. Qiang, "The impact of attitude feedback on the control performance and energy consumption in the path-following of unmanned rollers," SAE Tech. Paper 2020-01-5029, 2020, doi: 10.4271/2020-01-5029.

[26] Q. Xu, H. Xie, and K. Song, "The impact of control structure on the path-following control of unmanned compaction rollers," SAE Tech. Paper 2020-01-5030, 2020, doi: 10.4271/2020-01-5030.

[27] S. Chen, K. Song, L. Zhao, W. Xue, H. Xie, and Y. Huang, "On active disturbance rejection based path following control for unmanned roller," in *Proc. IEEE 58th Conf. Decis. Control (CDC)*, Nice, France, Dec. 2019, pp. 4791–4796.

[28] C. M. Roithmayr, D. H. Hodges, and P. Cross, "Formulation of equations of motion," in *Dynamics: Theory and Application of Kane's Method*. Cambridge, U.K.: Cambridge Univ. Press 2016, pp. 191–239.
[29] F. Braghin, F. Cheli, and S. Melzi, "Race driver model: Trajectory planning," in *III European Conference on Computational Mechanics: Solids, Structures and Coupled Problems in Engineering: Book of Abstracts*, C. A. Motasoares, J. A. C. Martins, H. C. Rodrigues, J. A. C. Ambrósio, C. A. B. Pina, C. M. Motasoares, E. B. R. Pereira, and J. Folgado, Eds. Dordrecht, The Netherlands: Springer, 2006, p. 764.
[30] S. Xu and H. Peng, "Design, analysis, and experiments of preview path tracking control for autonomous vehicles," *IEEE Trans. Intell. Transp. Syst.*, vol. 21, no. 1, pp. 48–58, Jan. 2020.
[31] K. van der El, D. M. Pool, M. R. M. van Paassen, and M. Mulder, "A unifying theory of driver perception and steering control on straight and winding roads," *IEEE Trans. Human-Mach. Syst.*, vol. 50, no. 2, pp. 165–175, Apr. 2020.
[32] I. Bae, J. H. Kim, and S. Kim, "Adaptive preview control of single-point path tracker for car-like delivery service robot," *Electron. Lett.*, vol. 56, no. 3, pp. 127–129, Feb. 2020.
[33] R. Liu and J. Duan, "A path tracking algorithm of intelligent vehicle by preview strategy," in *Proc. 32nd Chin. Control Conf.*, Xi'an, China, Jul. 2013, pp. 5630–5635.

MENG YANG received the B.S. degree in mechanical design, manufacturing, and automation, and the Ph.D. degree in mechanical engineering from Tongji University, Shanghai, China, in 2013 and 2019, respectively. He is currently a Postdoctoral Research Fellow with the Department of Control Science and Engineering, Tongji University. He has presided over the National Postdoctoral Program for Innovative Talents, the Shanghai Postdoctoral Excellence Program, and six enterprise projects. He is the author of more than ten academic articles in journals and seven inventions. His research interests include autonomous driving, path planning, and intelligent vehicle dynamics and control.

YONGMING BIAN received the M.S. degree in automotive engineering and the Ph.D. degree in mechanical engineering from Tongji University, Shanghai, China, in 1991 and 1999, respectively.

He is currently the Dean and a Professor with the School of Mechanical Engineering, Tongji University. He has presided over the National Key Research and Development Program, the National Natural Science Foundation, and more than 30 research projects of provincial and ministerial level. He has authored two textbooks, more than 100 academic articles, and over 40 inventions. His research interests include real-time network control theory and intelligent construction robot. He has received the Second Prize in National Scientific and Technological Progress Award, and 16 prizes of provincial and ministerial level.

GUANGJUN LIU received the M.S. degree in mechanical design and theory from the Harbin University of Science and Technology, Harbin, China, in 2004, and the Ph.D. degree in mechanical engineering from Shanghai Jiao Tong University, Shanghai, China, in 2007. He is currently a Professor with the School of Mechanical Engineering, Tongji University, Shanghai. He has presided over the National High Technology Research and Development Program, the National Natural Science Foundation, and more than 20 research projects of provincial and ministerial level. He has authored more than 50 academic articles. His research interests include intelligent construction robot and emergency rescue equipment.

HAO ZHANG received the M.S. degree in automatic control from Xi'an Jiaotong University, Xi'an, China, in 1987, and the Ph.D. degree in mechanical engineering from Shanghai Jiao Tong University, Shanghai, China, in 1990.

He is currently a Professor with the Department of Control Science and Engineering, Tongji University, Shanghai. He also serves as a Visiting Professor with The University of Melbourne. He has presided over the National High Technology Research and Development Program, the National Natural Science Foundation, and more than 30 research projects of provincial and ministerial level. He has authored over ten textbooks and more than 200 academic articles. His research interests include artificial intelligence and automatic control theory. He was a recipient of the Second Prize in National Scientific and Technological Progress Award, and more than 20 prizes of provincial and ministerial level.